ORGANIC CHEMISTRY FRONTIERS

RESEARCH ARTICLE

View Article Online
View Journal | View Issue

Open Access Article. Published on 12 October 2023. Downloaded on 8/2/2025 3:10:18 AM.
This article is licensed under a Creative Commons Attribution 3.0 Unported Licence.

Check for updates

Cite this: *Org. Chem. Front.*, 2023, **10**, 5876

Visible light-mediated hydrogen atom transfer and proton transfer for the conversion of (2-vinylaryl) methanol derivatives to aryl aldehydes or aryl ketones†

Jun Yan,[a] Ziqi Yu,[a] Hao-Zhao Wei,[a] Min Shi *[a,b] and Yin Wei *[b]

Received 9th August 2023,
Accepted 10th October 2023

DOI: 10.1039/d3qo01266b

rsc.li/frontiers-organic

In this paper, we report a photochemical strategy for the visible light-mediated efficient conversion of (2-vinylaryl)methanol derivatives to the corresponding aryl aldehydes or aryl ketones in moderate to excellent yields with broad substrate scope under mild conditions. This photochemical process takes place from the generation of the triplet state of olefins and involves 1,5-hydrogen atom transfer, enol tautomerization, and a subsequent proton transfer process. The plausible reaction mechanism has been verified by deuterium labeling and control experiments, kinetic and Stern–Volmer analyses, and DFT calculations.

Introduction

Visible light-mediated chemical transformations have become a powerful tool in synthetic chemistry[1] and materials science[2] for the efficient construction of novel chemical skeletons under mild conditions in the last decade. On the basis of visible light-mediated reaction modes of single electron transfer (SET) and energy transfer (EnT), various robust organic transformations can be achieved under mild conditions, such as C–H bond functionalizations,[3] C–C and C–X (X = heteroatom) bond formations as well as their selective cleavage and the subsequent downstream functionalizations and so on.[4] The SET pathway relies heavily on a redox process between a photosensitizer and a reaction substrate or a reaction intermediate,[5] so the excited-state photosensitizer often performs the role of an oxidant or a reductant. For example, in transition metal-catalyzed reductive coupling reactions,[6] the photoredox strategy is often used in place of a stoichiometric metal reductant, and hence the reaction can be performed under more environmentally-benign conditions. It is worth noting that the EnT reaction mode is also an effective way to obtain highly reactive intermediates in the excited state (or the ground state) under mild conditions.[7] These highly reactive excited intermediates often undergo pivotal chemical transformations that are not possible with regard to their corresponding ground states.

Olefins as unsaturated hydrocarbons are remarkably valuable synthetic scaffolds in organic synthetic chemistry.[8] Excited olefins allow for many chemical transformations such as atom transfer reactions,[9] [2 + 2] cyclizations,[10] and $E \rightarrow Z$ isomerizations[11] that cannot be realized in the ground state. Nevertheless, the direct excitation of most olefinic compounds *via* visible light irradiation is disfavored, basically due to the comparatively low absorption at longer wavelengths. In general, harsh UV light irradiation is required for the direct excitation of styryl organic molecules, which leads to negative impacts on the selectivity, functional group tolerance and general applicability of the reaction, as well as competitive and uncontrollable side reactions.[12,13] For example, the conversion of (2-(1-phenylvinyl)phenyl)methanol to the corresponding 2-(1-phenylethyl)benzaldehyde under UV irradiation was reported by Hornback's group in 1979 (Scheme 1a).[14] As shown in Scheme 1a, it must be emphasized here that due to the harsh UV irradiation, the photochemical reaction product was only obtained in 6.3% yield in the absence of a photosensitizer, and even with the addition of xanthone as a photosensitizer, the corresponding benzaldehyde was obtained only in 15.1% yield. The low yield is probably due to the Norrish-type reaction[15] of 2-(1-phenylethyl)benzaldehyde under UV light irradiation, which leads to the decomposition of the obtained product. Therefore, it is conceivable that the use of the recently

[a]*Key Laboratory for Advanced Materials and Institute of Fine Chemicals, School of Chemistry & Molecular Engineering, East China University of Science and Technology, 130 Meilong Road, Shanghai 200237, China. E-mail: mshi@mail.sioc.ac.cn*

[b]*State Key Laboratory of Organometallic Chemistry, Center for Excellence in Molecular Synthesis, Shanghai Institute of Organic Chemistry, University of Chinese Academy of Science, Chinese Academy of Sciences, 345 Lingling Road, Shanghai 200032, China. E-mail: mshi@mail.sioc.ac.cn, weiyin@sioc.ac.cn*

† Electronic supplementary information (ESI) available: Experimental procedures and characterization data of new compounds. See DOI: **https://doi.org/10.1039/d3qo01266b**

This journal is © the Partner Organisations 2023

Open Access Article. Published on 12 October 2023. Downloaded on 8/2/2025 3:10:18 AM.
This article is licensed under a Creative Commons Attribution 3.0 Unported Licence.

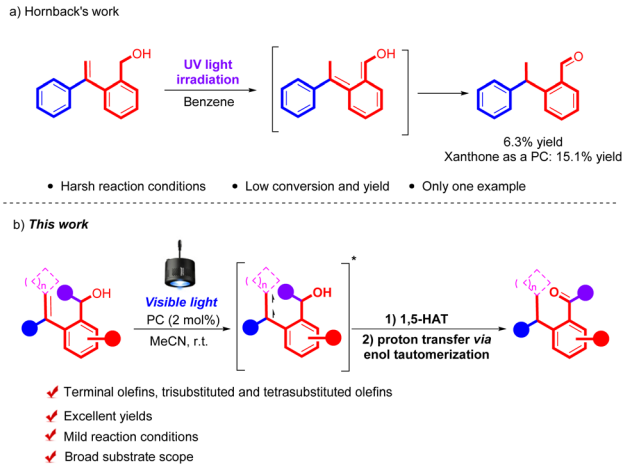

Scheme 1 Previous work and this work.

developed visible light-mediated strategy can avoid the further excitation of the formed aldehyde and realize an effective photochemical conversion of (2-vinylaryl)methanol derivatives to aryl aldehydes or aryl ketones.

Based on the above description and our previous work,[9c,d] we envisaged that the triplet state of (2-vinylaryl)methanol derivatives would be achieved through an EnT process upon visible light irradiation in corporation with a photocatalyst, in which the unprotected benzyloxy functional group could be used as a hydrogen atom transfer (HAT) partner and the subsequent enol interconversion isomerization as well as proton transfer would take place, resulting in an efficient conversion to aryl aldehydes or aryl ketones (Scheme 1b, this work). In this scenario, we anticipated that the desired product can be obtained in high yield along with broad substrate scope.

To test our working hypothesis, we started our investigation by using (2-(cyclopropylidene(phenyl)methyl)phenyl)methanol **1a** (0.2 mmol, 1.0 equiv.) as a substrate, Ir(dF-CF_3-ppy)$_2$(dtbbpy)PF_6 (2 mol%) as a photosensitizer, and degassed MeCN (2.0 mL) as the solvent under irradiation with 5 W blue LEDs for 12 hours under an argon atmosphere. To our delight, the desired aromatic aldehyde product **2a** was obtained in 94% isolated yield (Table 1, entry 1). However, when using photosensitizers such as [Ir(2′,4′-dF-5-CF_3-ppy)$_2$(bpy)]PF_6 having a slightly lower triplet state energy (Table 1, entry 2) and Ir(dFppy)$_2$pic having a higher triplet state energy (Table 1, entry 3) as the photocatalysts, **2a** was obtained in lower NMR yields of 31% and 25%, respectively. The use of *fac*-Ir(ppy)$_3$, [Ru(phen)$_3$](PF_6)$_2$, and [Ru(bpy)$_3$](PF_6)$_2$ as the photocatalysts, which have lower triplet state energies, did not give **2a** at all (Table 1, entries 4–6). When xanthone was used as a photosensitizer, the expected product **2a** was not detected (Table 1, entry 7). This is probably due to that xanthone (λ_{max} = 340 nm) is not absorbed in the visible light region.[16] Notably, this photosensitizer was used by Hornback's group in the photochemical synthesis of benzaldehyde. The solvent effects on the reaction outcome were then examined, including dichloromethane (Table 1, entry 8), tetrahydrofuran (Table 1, entry 9),

Table 1 Optimization of the reaction conditions[a,b]

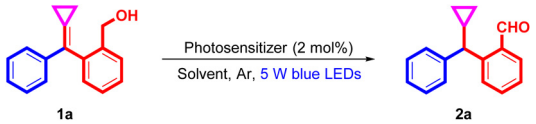

Entry	PC	E_T (kcal mol^{-1})	Solvent	Conc. [M]	Yield[b] (%)
1	Ir(dF-CF_3-ppy)2(dtbbpy)PF_6	60.8	MeCN	0.1	94[c]
2	[Ir(2′,4′-dF-5-CF_3-ppy)$_2$(bpy)]PF_6	60.4	MeCN	0.1	31
3	Ir(dFppy)$_2$pic	61.1	MeCN	0.1	25
4	*fac*-Ir(ppy)$_3$	57.8	MeCN	0.1	N.R
5	[Ru(phen)$_3$](PF_6)$_2$	48.4	MeCN	0.1	N.R
6	[Ru(bpy)$_3$](PF_6)$_2$	46.5	MeCN	0.1	N.R
7	Xanthone	74.3	MeCN	0.1	N.R
8	Ir(dF-CF_3-ppy)$_2$(dtbbpy)PF_6		DCM	0.1	24
9	Ir(dF-CF_3-ppy)$_2$(dtbbpy)PF_6		THF	0.1	29
10	Ir(dF-CF_3-ppy)$_2$(dtbbpy)PF_6		Toluene	0.1	65
11	Ir(dF-CF_3-ppy)$_2$(dtbbpy)PF_6		MeCN	0.05	85
12	Ir(dF-CF_3-ppy)$_2$(dtbbpy)PF_6		MeCN	0.2	68
13	None		MeCN	0.1	N.R
14[d]	Ir(dF-CF_3-ppy)$_2$(dtbbpy)PF_6		MeCN	0.1	N.R
15[e]	Ir(dF-CF_3-ppy)$_2$(dtbbpy)PF_6		MeCN	0.1	90

[a] Reaction conditions: **1a** (0.1 mmol) and PC (2 mol%) were added in degassed solvent (2.0 mL) under an Ar atmosphere for 12.0 h, in a sealed tube under 5 W blue LED light irradiation. [b] Yields were determined by ^{1}H NMR using 1,3,5-trimethoxybenzene as an internal standard. [c] Isolated yield. [d] No light. [e] Under 100 W blue LEDs for 6 h.

and toluene (Table 1, entry 10), and they afforded **2a** in reduced yields compared to MeCN. The substrate concentration did not have a significant impact on the yield of **2a** as shown in entries 11 and 12 of Table 1. Control experiments elucidated that the target product was not obtained in the absence of a photosensitizer (Table 1, entry 13) or under dark conditions (Table 1, entry 14). When a higher power lamp was used as the light source, it speeded up the rate of the reaction, but did not increase the yield (Table 1, entry 15).

Having determined the optimized conditions, the substrate scope of this newly developed photochemical reaction was investigated with a wide variety of substrates **1** and we found that most of them provided the corresponding arylaldehydes **2** smoothly in good to excellent yields (Table 2). For terminal olefins, substrates **1** with various substituted aryl groups as R^1 moieties, regardless of whether they had electron-donating or electron-withdrawing groups, were tolerated in the protocol, delivering the target products **2b–2g** in moderate to excellent yields ranging from 65% to 96%. Substrate **1h**, in which R^1 was a thienyl group, also afforded the corresponding arylaldehyde **2h** in 83% yield. We also examined the effects of substituents at the aryl alcohol moiety on the reaction outcome, revealing that substrates **1i–1n** having 4-Cl, 5-Cl, 4-Br, 5-Br, 4-Me, and 5-Me substituted aryl alcohols were all compatible in this transformation, providing the desired products **2i–2n** in moderate to good yields ranging from 57% to 92% yields. For Br and methyl substituents, changing the position from 5-substitution to 4-substitution induced over a 30% increase in yield (**2k** and **2l**, **2m** and **2n**). Therefore, we hypothesized that in

Open Access Article. Published on 12 October 2023. Downloaded on 8/2/2025 3:10:18 AM.
This article is licensed under a Creative Commons Attribution 3.0 Unported Licence.

Table 2 Substrate scope of **1**[a,b]

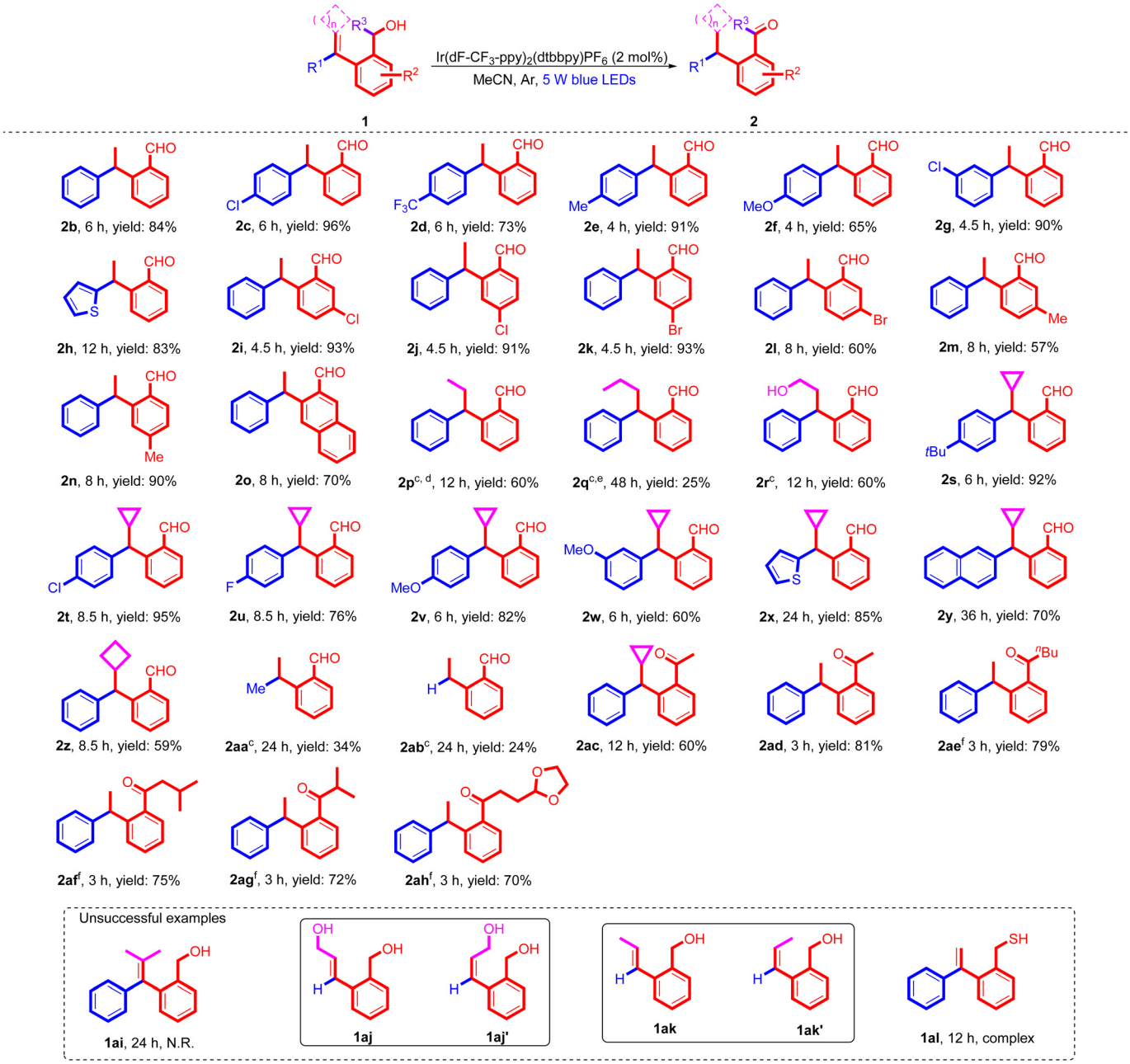

[a] Reaction conditions: **1** (0.2 mmol) and **PC** (2 mol%) were added in solvent (2.0 mL) under an Ar atmosphere, in a sealed tube under 5 W blue LED light irradiation. [b] Yield of the isolated products. [c] Using 100 W blue light irradiation. [d] The *E*/*Z* ratio of substrate **1p** is 4 : 1. [e] The *E*/*Z* ratio of substrate **1q** is 6 : 4. [f] A 6 : 1 mixture of MeCN and H_2O was used as the solvent.

terms of electronic effects, the Br and methyl substituents at the 4-position probably make the corresponding intermediate **IV** (shown in Scheme 4) unstable, thus leading to a decrease in yields (**2l** and **2m**). Substrate **1o** bearing a naphthalenemethanol unit as a HAT partner was also smoothly converted to the corresponding aldehyde **2o** in 70% yield under the standard conditions. When using substrates **1p**, **1q** and **1r** containing a trisubstituted olefinic moiety in this photochemical reaction, the corresponding products **2p**–**2r** were also obtained in moderate yields under 100 W blue light irradiation. For substrates **1p**, **1q**, and **1r** containing trisubstituted olefinic molecules, the *E*/*Z* isomerization occurred as a side reaction; thus, 100 W blue LED light was used to ensure that the 1,5-HAT process as a critical step was able to proceed more efficiently to give the desired products in moderate yields. The desired product **2p** was obtained in 60% yield when using **1p** (*E*/*Z* = 4/1) as a substrate. However, it is worth noting that the *E*/*Z* ratio of substrate **1q** is 6/4, and the *Z*-trisubstituted olefin **1q′** cannot be

 This journal is © the Partner Organisations 2023

Open Access Article. Published on 12 October 2023. Downloaded on 8/2/2025 3:10:18 AM.
This article is licensed under a Creative Commons Attribution 3.0 Unported Licence.

excited under the standard conditions due to its higher EnT energy,[11a] thus leading to a significant decrease in the yield of **2q** to 25% yield. Substrate **1r** with a free hydroxyl group was also tolerated in this protocol and the target product **2r** was obtained in 60% yield.

To further extend the scope of substrates **1**, a series of substrates bearing a methylenecyclopropane unit were used in this newly explored visible light-mediated photochemical reaction, and the corresponding products were obtained in good to excellent yields. For substrates **1s–1w**, in which R^1 was a substituted aryl group, the desired products **2s–2w** were also successfully obtained in good to high yields ranging from 60% to 95% regardless of whether the aryl group had an electron-withdrawing group or an electron-donating group. In addition, for substrates **1x** and **1y**, in which R^1 was a 2-thienyl group and a 2-naphthyl group, the reactions proceeded smoothly, delivering the desired products **2x** and **2y** in 85% and 70% yields, respectively, although a prolonged reaction time was required. This protocol also performed very well for substrate **1z** with a methylenecyclobutane unit, providing the desired aldehyde **2z** in 59% yield. Moreover, when substrates **1aa** (R^1 = Me) and **1ab** (R^1 = H) were used in the reaction, the corresponding aldehydes **2aa** and **2ab** were obtained in 34% and 24% yields, respectively, despite that the photochemical reactivity decreased dramatically. For the monoaryl substrates **1aa** and **1ab**, the excitation efficiency was lower than that of the diaryl substrates; thus, 100 W blue LED light is required.

Next, we turned our attention to examine the substrate scope of secondary alcohols. For substrates **1ac** and **1ad**, in which R^3 = Me, the reactions proceeded smoothly, furnishing the corresponding acetophenones **2ac** and **2ad** in moderate yields of 60% and 81%, respectively. When the methyl group was changed to a sterically hindered group such as an *n*-butyl, an isobutyl, or an isopropyl group or a 2-ethyl-1,3-dioxolane moiety, the desired products **2ae–2ah** were also obtained in moderate yields ranging from 70% to 79%. It is worth noting that in these cases, additional water was necessary to be added into the reaction system as a proton source to accelerate the proton transfer process efficiently.[17] Unfortunately, some limitations of this newly developed HAT and proton transfer reaction were observed for several substrates. For example, when non-cyclic tetrasubstituted olefin **1ai** was employed as a substrate, no reaction occurred under the standard conditions, probably due to the steric hindrance leading to the non-occurrence of the 1,5-HAT process. Furthermore, none of the desired products **2aj** and **2al** were detected for substrates **1aj** and **1ak** containing *E*-disubstituted olefins, and most of them isomerized to the corresponding *Z*-olefins **1aj′** and **1ak′** under the standard conditions.[11] For the monoaryl disubstituted olefins **1aj** and **1ak**, the desired reactions did not occur, probably due to that they were more difficult to excite, as well as the presence of *E*/*Z* isomerization. When the OH group was changed to the SH group (**1al**), the reaction system became complex.

To further investigate the reaction mechanism, a series of deuteration experiments and controlled experiments were carried out. First, the kinetic isotope effect of this photochemical reaction was determined using the mono-deuterated substrate [D_1]-**1a**, and $k_H/k_D \approx 5.7$ was obtained for the formation of [D_1]-**2a**, indicating that the C–H bond homolytic cleavage is involved in the rate-determining step (Scheme 2a) (see page S13 in the ESI†). Subsequently, the double-deuterated substrate [D_2]-**1a** was used in the reaction under the standard conditions, providing the target product [D_2]-**2a** in 33% yield along with >99% deuterium incorporation (Scheme 2b). These obtained results are consistent with our working assumption that the olefinic biradical species at the triplet state undergoes a 1,5-HAT process with the C(sp^3)–H bond at the benzylic alcohol position to give an open-shell biradical species. To clarify another benzylic proton source in the product, we carried out this reaction using substrate [D_1]-**1a′**, in which the alcoholic hydrogen atom was deuterated, giving the deuterated product in 91% yield along with 87% deuterium incorporation, suggesting that the benzylic proton of [D_1]-**2a′** indeed comes from the alcoholic hydrogen atom in the substrate (Scheme 2c). As shown in Scheme 2d, when the reaction was carried out using **1ae** as a substrate under the standard conditions in anhydrous MeCN, the reaction efficiency dropped down significantly, affording the desired product **2ae** in only 33% yield, and benzocyclobutane **3** was detected in 51% yield as a diastereomeric mixture, which was produced by [2 + 2] electrocyclization of the conjugated diene intermediate in the reaction.[9d] However, when the solvent was replaced with a mixture of MeCN and H_2O (6 : 1), the target product **1ae** was obtained in 78% yield as a sole product under otherwise identical conditions (Scheme 2e) (see Table 2 as well). This result suggests that the ambient H_2O in the reaction system is likely to accelerate the proton transfer process,[17] and as for sub-

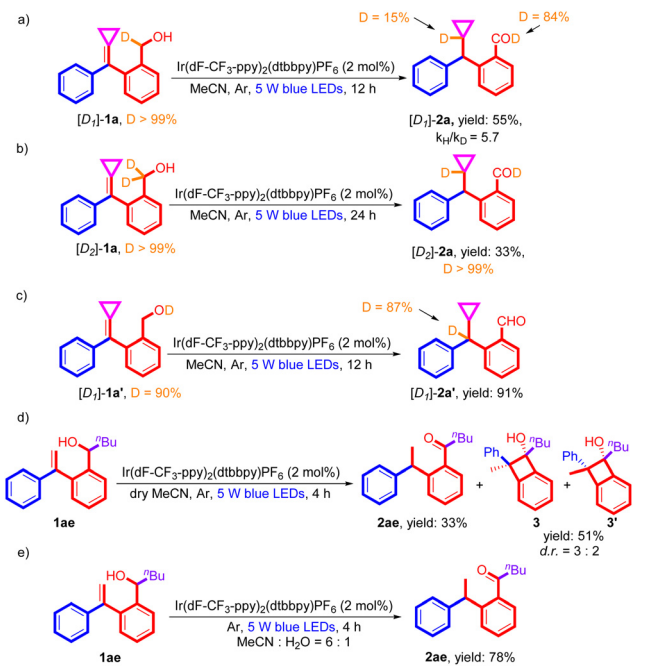

Scheme 2 Deuterium labeling and control experiments.

Open Access Article. Published on 12 October 2023. Downloaded on 8/2/2025 3:10:18 AM.
This article is licensed under a Creative Commons Attribution 3.0 Unported Licence.

strates bearing sterically large groups, the reaction efficiency can be improved.

To further elucidate the interaction details of substrate **1** and the photocatalyst Ir(dF-CF_3-ppy)$_2$(dtbbpy)PF_6, a fluorescence quenching experiment was performed using substrate **1a** with Ir(dF-CF_3-ppy)$_2$(dtbbpy)PF_6 (Fig. 1a) (see page S16 in the ESI†). From Stern–Volmer analysis, it can be seen that the emission of Ir(dF-CF_3-ppy)$_2$(dtbbpy)PF_6 was effectively quenched by substrate **1a**, suggesting that substrate **1a** may be photoexcited by the photosensitizer *via* an EnT pathway upon 5 W blue LED irradiation (Fig. 1b). The oxidation potential of substrate **1a** was determined by cyclic voltammetry as $E^{ox}_{p/2}$ = +1.75 V *vs.* SCE (Fig. 1c) (see page S17 in the ESI†), showing that it is impossible for substrate **1a** to undergo a SET process with the used photosensitizer (E_{red} (*Ir^{III}/Ir^{II}) = 1.21 V *vs.* SCE). For the terminal olefinic substrate **1l**, we also determined its oxidation potential as $E^{ox}_{p/2}$ = +1.35 V *vs.* SCE, suggesting that all these olefinic substrates undergo an EnT process under the standard conditions (see page S17 in the ESI†). Meanwhile, the light–dark interval experiments (Fig. 1d) and the quantum yield of 0.13 for this photochemical reaction (see page S18 in the ESI†) indicated that continuous visible light irradiation is an essential element in the product formation process and the radical chain process might not be involved in the turnover process.

DFT calculations were performed to gain insight into the reaction mechanism. All calculations were performed at the SMD(CH_3CN)/M06/def2tzvpp//M06/def2svp level with the Gaussian 16 program.[18] The solvation Gibbs free energy profile in acetonitrile for the suggested reaction pathway is shown in Scheme 3 (see page S174 in the ESI†). The first triplet-state of **1a** (**int-1a**) lies higher than the ground state of **1a** by 44.5 kcal mol^{-1}, and the Ir(dF-CF_3-ppy)$_2$(dtbbpy)PF_6 in the excited state (60.8 kcal mol^{-1}) can promote the formation of **int-1a** *via* an EnT pathway. Subsequently, **int-1a** undergoes 1,5-HAT *via* **ts-1a** to form the open-shell biradical intermediate **int-2a** (20.8 kcal mol^{-1}) with a reaction energy barrier of 11.8 kcal mol^{-1}. The intersystem crossing of **int-2a** gives the closed-shell conjugated diene intermediate **int-3a** (18.9 kcal mol^{-1}). Once **int-3a** is generated, the subsequent proton transfer takes place to generate the corresponding product **2a** (−17.2 kcal mol^{-1}) *via* **ts-2a** with a reaction barrier of 0.5 kcal mol^{-1}. We also examined the reaction barrier (**ts-3a**, $\Delta G^{\ddagger}$ = 10.4 kcal mol^{-1}) for **int-3a** to undergo electrocyclization to form benzocyclobutane **3a** (3.0 kcal mol^{-1}). The results show that the pathway to generate benzocyclobutane is unfavourable. For the reaction of the terminal olefin **1b**, we also performed DFT calculations; the calculation results are shown in Scheme 3b and they are similar to those of substrate **1a**, which undergoes the 1,5-HAT process and the subsequent proton transfer process. DFT calculations for the reaction of the substrate (**1ae**) having a secondary alcohol moiety were also performed (Scheme 3c). First, the energy transfer of the photosensitiser in the excited state occurs to obtain the

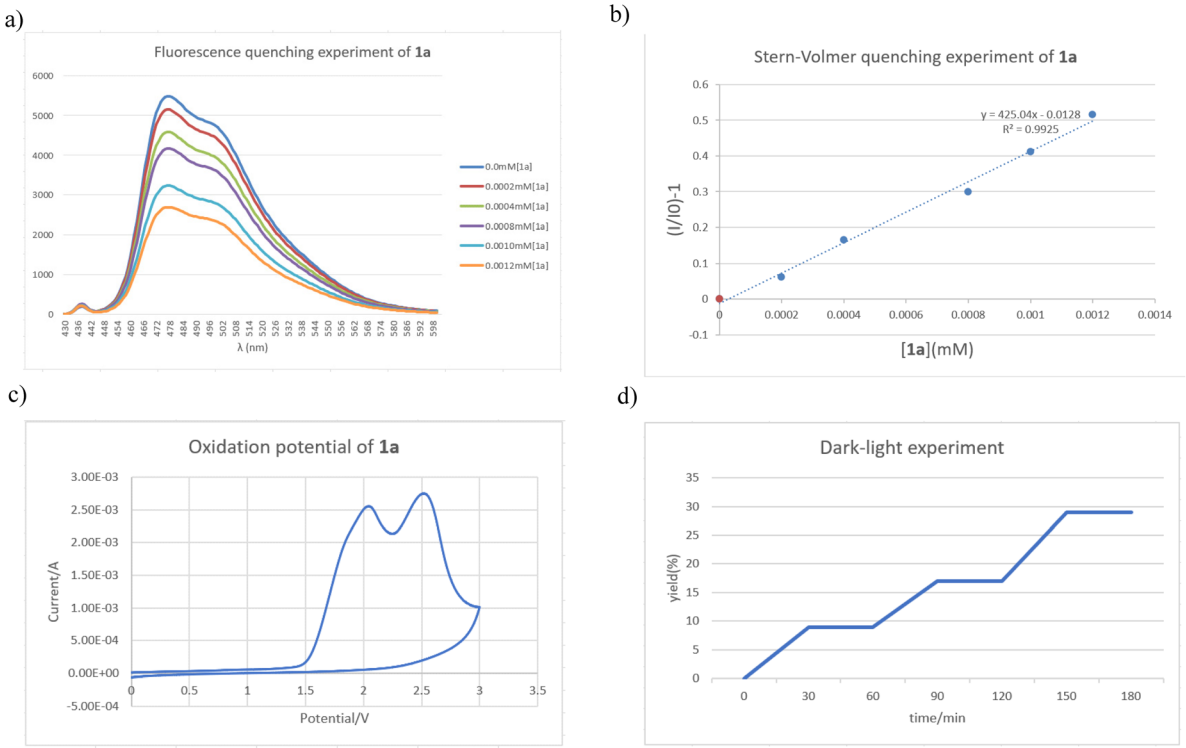

Fig. 1 Mechanistic studies. (a) An appropriate amount of **1a** was added to a 0.001 M photocatalyst solution in MeCN under an argon atmosphere and the emission from the sample was collected; (b) Stern–Volmer studies; (c) a solution of the substrate **1a** in MeCN (0.1 M) was tested with 0.1 M Bu_4NPF_6 as the supporting electrolyte. Scan rate = 0.1 V s^{-1}; (d) light on/off experiments.

Open Access Article. Published on 12 October 2023. Downloaded on 8/2/2025 3:10:18 AM.
This article is licensed under a Creative Commons Attribution 3.0 Unported Licence.

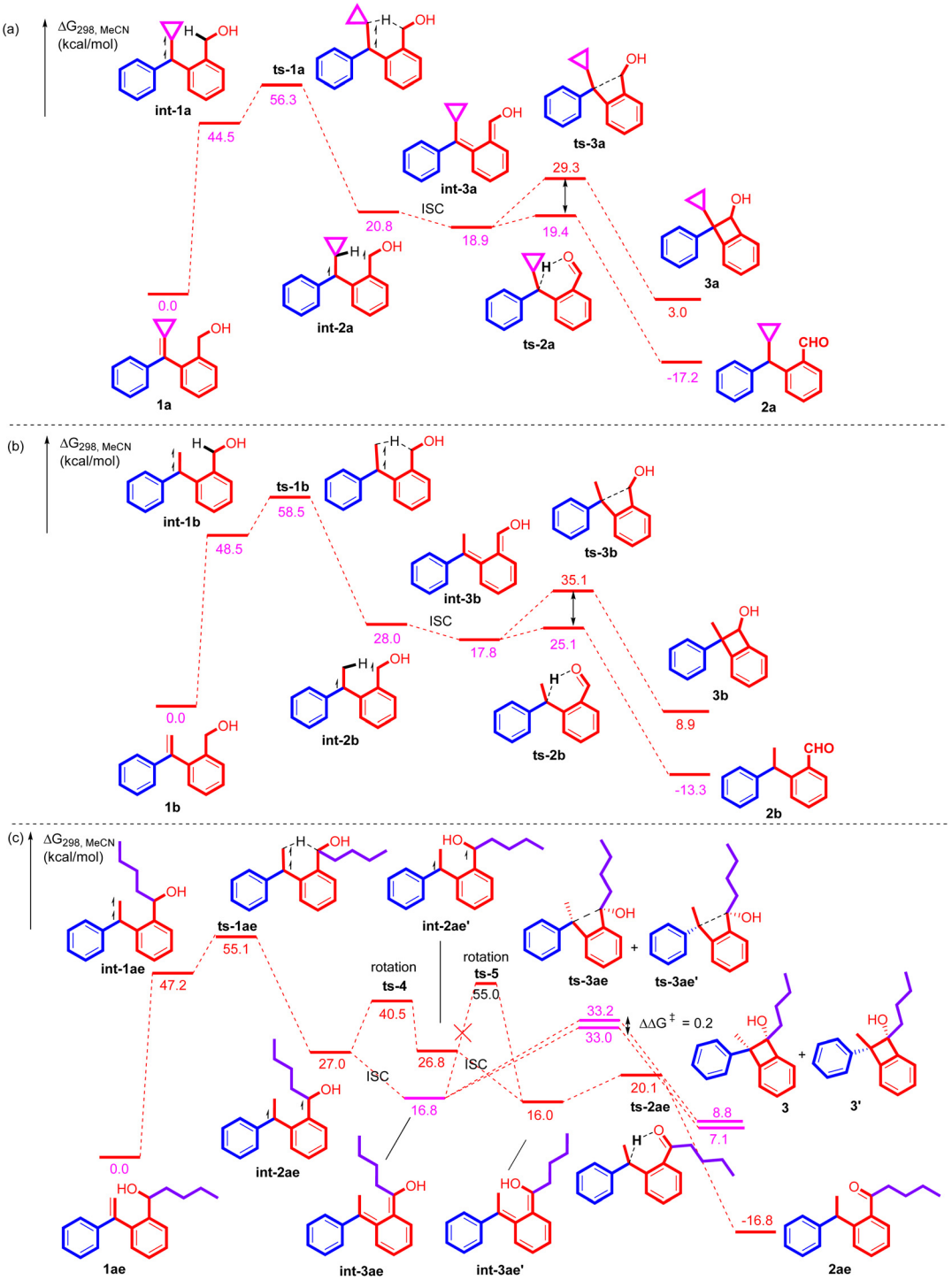

Scheme 3 (a) DFT calculations on the reaction of **1a**; (b) DFT calculations on the reaction of **1b**; (c) DFT calculations on the reaction of **1ae**.

excited-state intermediate **int-1ae**, and the energy of this state is 47.2 kcal mol^{-1} higher than that of **1a**. Subsequently, **int-1ae** undergoes 1,5-HAT across a low reaction energy barrier (**ts-1ae**, $\Delta G^{\ddagger}$ = 7.9 kcal mol^{-1}) to form the biradical intermediate **int-2ae** (27.0 kcal mol^{-1}). Considering that butyl is a sterically hindered group, we calculated the rotational energy barrier for the transformation of **int-2ae** into **int-2ae′**, which is 13.5 kcal mol^{-1} and indicates that both **int-2ae** and **int-2ae′** can exist in the reaction system. DFT calculations show that **int-3ae′** cannot be obtained through the direct rotation of **int-3ae** because the rotation barrier is 38.2 kcal mol^{-1} which is difficult to overcome under the standard reaction conditions. Finally, **int-2ae′** undergoes proton transfer *via* **ts-2ae** ($\Delta G^{\ddagger}$ = 4.1 kcal mol^{-1}) to produce the corresponding ketone **2ae**; the

Open Access Article. Published on 12 October 2023. Downloaded on 8/2/2025 3:10:18 AM.
This article is licensed under a Creative Commons Attribution 3.0 Unported Licence.

intermediate **int-2ae** undergoes electrocyclization *via* **ts-3ae** or **ts3–3ae′** to give a pair of diastereomers **3** and **3′**, ($\Delta\Delta G^{\ddagger}$ = 0.2 kcal mol^{-1}) which is basically in line with the dr value obtained in the experiment (dr = 3 : 2, see Scheme 2d).

Based on the previous literature[9] and our own experimental results above, a possible mechanism for this photochemical conversion is depicted in Scheme 4. First, the photosensitizer enters the excited state under visible light irradiation, which is quenched by substrate **1a** through an EnT pathway to revert to the ground state, and **1a** is converted to its triplet state as a biradical species **I**. Subsequently, the species **I** abstracts the hydrogen atom at the benzylic alcohol position *via* a 1,5-HAT process to produce the open-shell biradical intermediate **II**, followed by intersystem crossing to give the closed-shell conjugated diene intermediate **III**. Finally, intermediate **IV** is formed by an enol intercalative isomerization, and it undergoes a proton transfer process to give the corresponding product **2a**.

To demonstrate the synthetic utility of this newly explored photochemical reaction, a gram-scale reaction of **1a** was executed and this reaction worked well, affording **2a** in 91% yield (Scheme 5). Subsequently, **2a** and **2b** were subjected to a series of transformations under different reaction conditions. First, **2a** underwent a Witting reaction in THF with the *in situ* generated phosphonium ylide to produce the corresponding substituted styrene **4** in 90% yield. Considering that product **2a** contains an unactivated cyclopropyl group, an attempt was made to achieve ring-opening 1,3-hydroboration of cyclopropane in DCM at room temperature in the presence of phenylsilane and boron tribromide according to the previous literature;[19] however, the corresponding benzyl bromide **5** was produced in 31% yield without the formation of the cyclopropane ring-opened product under the standard conditions. Next, substituted benzaldoxime **6** was obtained in 60% yield upon treating **2a** with 1.25 equiv. of $NH_2OH{\cdot}HCl$ and 2.50 equiv. of CH_3COONa in $HCOOH/H_2O$ (6/4) at 80 °C. Moreover, according to the previous literature,[20] products **2a** and **2b** were smoothly transformed into trisubstituted pyridines **7** and **8** under the treatment with acetophenone and an ammonium salt at 130 °C in PhCl in the presence of 3 equiv. of DMSO and molecular oxygen (1.0 atm). In addition, the Knoevenagel reaction of product **2b** with dimethyl malonate provided the corresponding condensation product **9** in 84% yield (Scheme 5).

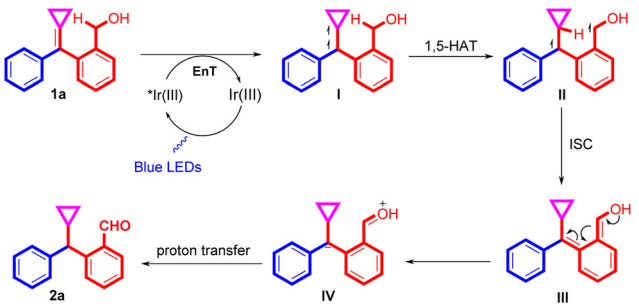

Scheme 4 A possible mechanism.

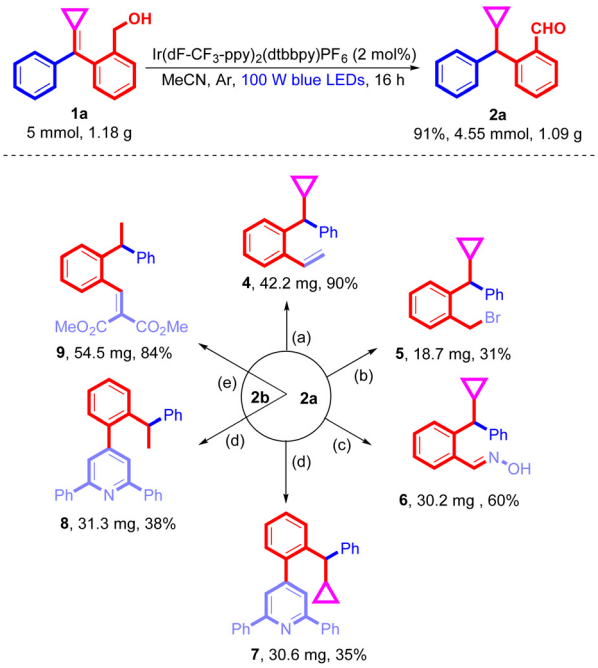

Scheme 5 Gram scale and product transformations. (a) **2a** (0.2 mmol), *t*-BuOK (0.40 mmol, 2.0 equiv., 1.0 mol L^{-1}), methyltriphenylphosphonium bromide (0.40 mmol, 2.0 equiv.), DCM, r.t.; (b) **2a** (0.20 mmol), phenylsilane (0.24 mmol, 1.2 equiv.), boron tribromide (0.24 mmol, 1.2 equiv., 0.24 mL of 1.0 M solution in DCM), DCM, r.t.; (c) **2a** (0.20 mmol), $NH_2OH{\cdot}HCl$ (0.24 mmol, 1.2 equiv.), CH_3COONa (0.24 mmol, 1.2 equiv.), $HCOOH/H_2O$ (2.0 mL, 3 : 2), 80 °C; (d) **2a** (0.20 mmol, 1.0 equiv.) or **2b** (0.20 mmol), phenylacetophenone (0.60 mmol, 3.0 equiv.), NH_4I (0.40 mmol, 2 equiv.), DMSO (0.60 mmol, 3.0 equiv.), molecular oxygen (1.0 atm), PhCl, 130 °C; (e) **2b** (0.20 mmol), dimethyl malonate (0.40 mmol, 2 equiv.) AcOH (10 mol%), piperazine (10 mol%), toluene, 100 °C.

Conclusions

In conclusion, we have explored a novel approach for the transformation of (2-vinylaryl)methanol derivatives into the corresponding aryl aldehydes or aryl ketones in moderate to excellent yields under mild conditions *via* visible light-mediated 1,5-HAT, enol interconversion and proton transfer processes with wide substrate scope. Deuterium labeling and kinetic analysis experiments verify that the HAT process takes place at the excited triplet state of olefins and the homolytic cleavage of the C–H bond is the rate-limiting step in this photochemical reaction. Meanwhile, another enol tautomerization-involved proton transfer process is also involved in this photochemical reaction. In addition, the control experiments have demonstrated that the presence of water in the reaction system can accelerate the proton transfer process and the possibility that the photoreaction may involve a radical chain process has also been ruled out by on and off light experiments and the determination of the quantum yield. This novel photochemical strategy further broadens the reaction patterns of visible light-mediated reactions of excited-state olefins. Further investigations based on the visible light-mediated conversion of

Open Access Article. Published on 12 October 2023. Downloaded on 8/2/2025 3:10:18 AM.
This article is licensed under a Creative Commons Attribution 3.0 Unported Licence.

triplet-state compounds and their applications in materials science and synthetic chemistry such as in natural product total synthesis and medicinal chemistry are currently underway.

Author contributions

Yan, J. and Wei, H. Z. contributed to the investigation. Yu, Z. Q., Wei, Y., and Yan, J. contributed to the calculations. Yan, J., Wei, Y., and Shi, M. contributed to conceptualization and writing – original draft.

Conflicts of interest

There are no conflicts to declare.

Acknowledgements

We are grateful for the financial support from the National Key R & D Program of China (2022YFC2303100), the National Natural Science Foundation of China (21372250, 21121062, 21302203, 20732008, 21772037, 21772226, 21861132014, 91956115 and 22171078), a project supported by the Shanghai Municipal Science and Technology Major Project (Grant No. 2018SHZDZX03) and the Fundamental Research Funds for the Central Universities 222201717003.

References

1 (*a*) Q. Liu and L.-Z. Wu, Recent Advances in Visible-Light-Driven Organic Reactions, *Natl. Sci. Rev.*, 2017, **4**, 359–380; (*b*) A. K. Bagdi, M. Rahman, D. Bhattacherjee, G. V. Zyryanov, S. Ghosh, O. N. Chupakhin and A. Hajra, Visible Light Promoted Cross-Dehydrogenative Coupling: A Decade Update, *Green Chem.*, 2020, **22**, 6632–6681; (*c*) S. P. Pitre and L. E. Overman, Strategic Use of Visible-Light Photoredox Catalysis in Natural Product Synthesis, *Chem. Rev.*, 2022, **122**, 1717–1751; (*d*) Y.-Z. Cheng, Z. Feng, X. Zhang and S.-L. You, Visible-Light Induced Dearomatization Reactions, *Chem. Soc. Rev.*, 2022, **51**, 2145–2170; (*e*) H.-Z. Wei, M. Shi and Y. Wei, Visible-Light-Induced Reactions of Methylenecyclopropanes (MCPs), *Chem. Commun.*, 2023, **59**, 2726–2738.

2 (*a*) H. K. Bisoyi and Q. Li, Light-Driven Liquid Crystalline Materials: From Photo-Induced Phase Transitions and Property Modulations to Applications, *Chem. Rev.*, 2016, **116**, 15089–15166; (*b*) G. Mamba and A. K. Mishra, Graphitic Carbon Nitride (g-C_3N_4) Nanocomposites: A New and Exciting Generation of Visible Light Driven Photocatalysts for Environmental Pollution Remediation, *Appl. Catal., B*, 2016, **198**, 347–377; (*c*) J. You, Y. Guo, R. Guo and X. Liu, A Review of Visible Light-Active Photocatalysts for Water Disinfection: Features and Prospects, *Chem. Eng. J.*, 2019, **373**, 624–641; (*d*) R. Weinstain, T. Slanina, D. Kand and P. Klán, Visible-to-NIR-Light Activated Release: From Small Molecules to Nanomaterials, *Chem. Rev.*, 2020, **120**, 13135–13272; (*e*) Z. Zhang, J. Jia, Y. Zhi, S. Ma and X. Liu, Porous Organic Polymers for Light-Driven Organic Transformations, *Chem. Soc. Rev.*, 2022, **51**, 2444–2490.

3 (*a*) D. C. Fabry and M. Rueping, Merging Visible Light Photoredox Catalysis with Metal Catalyzed C–H Activations: On the Role of Oxygen and Superoxide Ions as Oxidants, *Acc. Chem. Res.*, 2016, **49**, 1969–1979; (*b*) Q.-Y. Meng, T. E. Schirmer, A. L. Berger, K. Donabauer and B. König, Photocarboxylation of Benzylic C–H Bonds, *J. Am. Chem. Soc.*, 2019, **141**, 11393–11397; (*c*) T. Kawasaki, N. Ishida and M. Murakami, Dehydrogenative Coupling of Benzylic and Aldehydic C–H Bonds, *J. Am. Chem. Soc.*, 2020, **142**, 3366–3370; (*d*) L. Capaldo, D. Ravelli and M. Fagnoni, Direct Photocatalyzed Hydrogen Atom Transfer (HAT) for Aliphatic C–H Bonds Elaboration, *Chem. Rev.*, 2022, **122**, 1875–1924; (*e*) E. Le Saux, M. Zanini and P. Melchiorre, Photochemical Organocatalytic Benzylation of Allylic C–H Bonds, *J. Am. Chem. Soc.*, 2022, **144**, 1113–1118; (*f*) H. Cao, D. Kong, L.-C. Yang, S. Chanmungkalakul, T. Liu, J. L. Piper, Z. Peng, L. Gao, X. Liu, X. Hong and J. Wu, Brønsted Acid-Enhanced Direct Hydrogen Atom Transfer Photocatalysis for Selective Functionalization of Unactivated C(Sp^3)–H Bonds, *Nat. Synth.*, 2022, **1**, 79803.

4 (*a*) K. Chen, N. Berg, R. Gschwind and B. König, Selective Single C(Sp^3)–F Bond Cleavage in Trifluoromethylarenes: Merging Visible-Light Catalysis with Lewis Acid Activation, *J. Am. Chem. Soc.*, 2017, **139**, 18444–18447; (*b*) W. Shu, A. Genoux, Z. Li and C. Nevado, γ-Functionalizations of Amines through Visible-Light-Mediated, Redox-Neutral C–C Bond Cleavage, *Angew. Chem., Int. Ed.*, 2017, **56**, 10521–10524; (*c*) S. T. Nguyen, E. A. McLoughlin, J. H. Cox, B. P. Fors and R. R. Knowles, Depolymerization of Hydroxylated Polymers via Light-Driven C–C Bond Cleavage, *J. Am. Chem. Soc.*, 2021, **143**, 12268–12277; (*d*) X. Yu, M. Lübbesmeyer and A. Studer, Oligosilanes as Silyl Radical Precursors through Oxidative Si–Si Bond Cleavage Using Redox Catalysis, *Angew. Chem., Int. Ed.*, 2021, **60**, 675–679; (*e*) X.-Y. Yu, J.-R. Chen and W.-J. Xiao, Visible Light-Driven Radical-Mediated C–C Bond Cleavage/Functionalization in Organic Synthesis, *Chem. Rev.*, 2021, **121**, 506–561; (*f*) C.-H. Qu, X. Yan, S.-T. Li, J.-B. Liu, Z.-G. Xu, Z.-Z. Chen, D.-Y. Tang, H.-X. Liu and G.-T. Song, Visible Light-Mediated Metal-Free Alkyl Suzuki–Miyaura Coupling of Alkyl Halides and Alkenylboronic Acids/Esters: A Green Method for the Synthesis of Allyl Difluoride Derivatives, *Green Chem.*, 2023, **25**, 3453–3461; (*g*) X.-S. Zhou, Z. Zhang, W.-Y. Qu, X.-P. Liu, W.-J. Xiao, M. Jiang and J.-R. Chen, Asymmetric [3 + 2] Photocycloaddition of β-Keto Esters and Vinyl Azides by Dual Photoredox/Nickel Catalysis, *J. Am. Chem. Soc.*, 2023, **145**, 12233–12243; (*h*) X. Jiang, W. Xiong, S. Deng, F.-D. Lu, Y. Jia, Q. Yang, L.-Y. Xue, X. Qi, J. A. Tunge, L.-Q. Lu and

Open Access Article. Published on 12 October 2023. Downloaded on 8/2/2025 3:10:18 AM.
This article is licensed under a Creative Commons Attribution 3.0 Unported Licence.

W.-J. Xiao, Construction of Axial Chirality via Asymmetric Radical Trapping by Cobalt under Visible Light, *Nat. Catal.*, 2022, **5**, 788–797; (*i*) Q. Li, P. Dai, H. Tang, M. Zhang and J. Wu, Photomediated Reductive Coupling of Nitroarenes with Aldehydes for Amide Synthesis, *Chem. Sci.*, 2022, **13**, 9361–9365.

5 (*a*) A. R. Allen, E. A. Noten and C. R. J. Stephenson, Aryl Transfer Strategies Mediated by Photoinduced Electron Transfer, *Chem. Rev.*, 2022, **122**, 2695–2751; (*b*) A. Y. Chan, I. B. Perry, N. B. Bissonnette, B. F. Buksh, G. A. Edwards, L. I. Frye, O. L. Garry, M. N. Lavagnino, B. X. Li, Y. Liang, E. Mao, A. Millet, J. V. Oakley, N. L. Reed, H. A. Sakai, C. P. Seath and D. W. C. MacMillan, Metallaphotoredox: The Merger of Photoredox and Transition Metal Catalysis, *Chem. Rev.*, 2022, **122**, 1485–1542; (*c*) J. Liu, L.-Q. Lu, Y. Luo, W. Zhao, P.-C. Sun, W. Jin, X. Qi, Y. Cheng and W.-J. Xiao, Photoredox-Enabled Chromium-Catalyzed Alkene Diacylations, *ACS Catal.*, 2022, **12**, 1879–1885; (*d*) L.-H. Li, H.-Z. Wei, Y. Wei and M. Shi, The Morita–Baylis–Hillman Reaction for Non-Electron-Deficient Olefins Enabled by Photoredox Catalysis, *Chem. Sci.*, 2022, **13**, 1478–1483; (*e*) Q. Li, X. Gu, Y. Wei and M. Shi, Visible-Light-Induced Indole Synthesis *via* Intramolecular C–N Bond Formation: Desulfonylative C(Sp^2)–H Functionalization, *Chem. Sci.*, 2022, **13**, 11623–11632.

6 (*a*) Y.-L. Li, W.-D. Li, Z.-Y. Gu, J. Chen and J.-B. Xia, Photoredox Ni-Catalyzed Branch-Selective Reductive Coupling of Aldehydes with 1,3-Dienes, *ACS Catal.*, 2020, **10**, 1528–1534; (*b*) Y.-L. Li, S.-Q. Zhang, J. Chen and J.-B. Xia, Highly Regio- and Enantioselective Reductive Coupling of Alkynes and Aldehydes via Photoredox Cobalt Dual Catalysis, *J. Am. Chem. Soc.*, 2021, **143**, 7306–7313; (*c*) S. H. Lau, M. A. Borden, T. J. Steiman, L. S. Wang, M. Parasram and A. G. Doyle, Ni/Photoredox-Catalyzed Enantioselective Cross-Electrophile Coupling of Styrene Oxides with Aryl Iodides, *J. Am. Chem. Soc.*, 2021, **143**, 15873–15881; (*d*) H. Xie and B. Breit, Organophotoredox/Ni-Cocatalyzed Allylation of Allenes: Regio- and Diastereoselective Access to Homoallylic Alcohols, *ACS Catal.*, 2022, **12**, 3249–3255.

7 (*a*) F. S. Kalthoff, M. J. James, M. Teders, L. Pitzer and F. Glorius, Energy Transfer Catalysis Mediated by Visible Light: Principles, Applications, Directions, *Chem. Soc. Rev.*, 2018, **47**, 7190–7202; (*b*) Q. Zhou, Y. Zou, L. Lu and W. Xiao, Visible–Light–Induced Organic Photochemical Reactions through Energy–Transfer Pathways, *Angew. Chem., Int. Ed.*, 2019, **58**, 1586–1604; (*c*) F. S. Kalthoff and F. Glorius, Triplet Energy Transfer Photocatalysis: Unlocking the Next Level, *Chem*, 2020, **6**, 1888–1903; (*d*) H. Jung, H. Keum, J. Kweon and S. Chang, Tuning Triplet Energy Transfer of Hydroxamates as the Nitrene Precursor for Intramolecular C(Sp^3)–H Amidation, *J. Am. Chem. Soc.*, 2020, **142**, 5811–5818; (*e*) M. Zhu, X. Zhang, C. Zheng and S.-L. You, Visible-Light-Induced Dearomatization via [2 + 2] Cycloaddition or 1,5-Hydrogen Atom Transfer: Divergent Reaction Pathways of Transient Diradicals, *ACS Catal.*, 2020, **10**, 12618–12626; (*f*) J. Guo, Y. Chen, C. Wang, Q. He, X. Yang, T. Ding, K. Zhang, R. Ci, B. Chen, C. Tung and L. Wu, Direct Excitation of Aldehyde to Activate the C(Sp^2)–H Bond by Cobaloxime Catalysis toward Fluorenones Synthesis with Hydrogen Evolution, *Angew. Chem., Int. Ed.*, 2023, **62**, e202214944; (*g*) M. J. Oddy, D. A. Kusza and W. F. Petersen, Visible-Light Mediated Metal-Free 6π-Photocyclization of *N*-Acrylamides: Thioxanthone Triplet Energy Transfer Enables the Synthesis of 3,4-Dihydroquinolin-2-Ones, *Org. Lett.*, 2021, **23**, 8963–8967.

8 (*a*) Z. Dong, Z. Ren, S. J. Thompson, Y. Xu and G. Dong, Transition-Metal-Catalyzed C–H Alkylation Using Alkenes, *Chem. Rev.*, 2017, **117**, 9333–9403; (*b*) L. Massaro, J. Zheng, C. Margarita and P. G. Andersson, Enantioconvergent and Enantiodivergent Catalytic Hydrogenation of Isomeric Olefins, *Chem. Soc. Rev.*, 2020, **49**, 2504–2522; (*c*) H. Jiang and A. Studer, Intermolecular Radical Carboamination of Alkenes, *Chem. Soc. Rev.*, 2020, **49**, 1790–1811; (*d*) S. Engl and O. Reiser, Copper-Photocatalyzed ATRA Reactions: Concepts, Applications, and Opportunities, *Chem. Soc. Rev.*, 2022, **51**, 5287–5299; (*e*) W. Lee, I. Park and S. Hong, Photoinduced Difunctionalization with Bifunctional Reagents Containing N-Heteroaryl Moieties, *Sci. China: Chem.*, 2023, **66**, 1688–1700.

9 (*a*) W. Ding, C. C. Ho and N. Yoshikai, Energy-Transfer-Mediated Cyclization of 2-(1-Arylvinyl)Benzaldehydes to Anthracen-9-(10 *H*)-Ones, *Org. Lett.*, 2019, **21**, 1202–1206; (*b*) T. Peez, V. Schmalz, K. Harms and U. Koert, Synthesis of Naphthocyclobutenes from α-Naphthyl Acrylates by Visible-Light Energy-Transfer Catalysis, *Org. Lett.*, 2019, **21**, 4365–4369; (*c*) J. Liu, Y. Wei and M. Shi, Direct Activation of a Remote C(Sp^3)–H Bond Enabled by a Visible–Light Photosensitized Allene Moiety, *Angew. Chem., Int. Ed.*, 2021, **60**, 12053–12059; (*d*) J. Liu, T. Hao, L. Qian, M. Shi and Y. Wei, Construction of Benzocyclobutenes Enabled by Visible–Light–Induced Triplet Biradical Atom Transfer of Olefins, *Angew. Chem., Int. Ed.*, 2022, **61**, e202204515; (*e*) Y. Xiong, J. Großkopf, C. Jandl and T. Bach, Visible Light–Mediated Dearomative Hydrogen Atom Abstraction/Cyclization Cascade of Indoles, *Angew. Chem., Int. Ed.*, 2022, **61**, e202200555; (*f*) M. J. Oddy, D. A. Kusza, R. G. Epton, J. M. Lynam, W. P. Unsworth and W. F. Petersen, Visible–Light–Mediated Energy Transfer Enables the Synthesis of B–Lactams via Intramolecular Hydrogen Atom Transfer, *Angew. Chem., Int. Ed.*, 2022, **61**, e202213086.

10 (*a*) P. Franceschi, S. Cuadros, G. Goti and L. Dell'Amico, Mechanisms and Synthetic Strategies in Visible Light–Driven [2 + 2]–Heterocycloadditions, *Angew. Chem., Int. Ed.*, 2023, **62**, e202217210; (*b*) A. Tröster, R. Alonso, A. Bauer and T. Bach, Enantioselective Intermolecular [2 + 2] Photocycloaddition Reactions of 2(1 *H*)-Quinolones Induced by Visible Light Irradiation, *J. Am. Chem. Soc.*, 2016, **138**, 7808–7811; (*c*) J. Zhao, J. L. Brosmer, Q. Tang, Z. Yang, K. N. Houk, P. L. Diaconescu and O. Kwon,

 This journal is © the Partner Organisations 2023

Open Access Article. Published on 12 October 2023. Downloaded on 8/2/2025 3:10:18 AM.
This article is licensed under a Creative Commons Attribution 3.0 Unported Licence.

Intramolecular Crossed [2 + 2] Photocycloaddition through Visible Light-Induced Energy Transfer, *J. Am. Chem. Soc.*, 2017, **139**, 9807–9810; (*d*) M. Zhu, C. Zheng, X. Zhang and S.-L. You, Synthesis of Cyclobutane-Fused Angular Tetracyclic Spiroindolines via Visible-Light-Promoted Intramolecular Dearomatization of Indole Derivatives, *J. Am. Chem. Soc.*, 2019, **141**, 2636–2644; (*e*) M. S. Oderinde, E. Mao, A. Ramirez, J. Pawluczyk, C. Jorge, L. A. M. Cornelius, J. Kempson, M. Vetrichelvan, M. Pitchai, A. Gupta, A. K. Gupta, N. A. Meanwell, A. Mathur and T. G. M. Dhar, Synthesis of Cyclobutane-Fused Tetracyclic Scaffolds via Visible-Light Photocatalysis for Building Molecular Complexity, *J. Am. Chem. Soc.*, 2020, **142**, 3094–3103; (*f*) R. Kleinmans, T. Pinkert, S. Dutta, T. O. Paulisch, H. Keum, C. G. Daniliuc and F. Glorius, Intermolecular [2π+2σ]-Photocycloaddition Enabled by Triplet Energy Transfer, *Nature*, 2022, **605**, 477–482.

11 (*a*) K. Singh, S. J. Staig and J. D. Weaver, Facile Synthesis of *Z* -Alkenes via Uphill Catalysis, *J. Am. Chem. Soc.*, 2014, **136**, 5275–5278; (*b*) A. Singh, C. J. Fennell and J. D. Weaver, Photocatalyst Size Controls Electron and Energy Transfer: Selectable *E*/*Z* Isomer Synthesis via C–F Alkenylation, *Chem. Sci.*, 2016, **7**, 6796–6802; (*c*) W. Cai, H. Fan, D. Ding, Y. Zhang and W. Wang, Synthesis of *Z* -Alkenes *via* Visible Light Promoted Photocatalytic $E \rightarrow Z$ Isomerization under Metal-Free Conditions, *Chem. Commun.*, 2017, **53**, 12918–12921; (*d*) H. Li, H. Chen, Y. Zhou, J. Huang, J. Yi, H. Zhao, W. Wang and L. Jing, Selective Synthesis of *Z* –Cinnamyl Ethers and Cinnamyl Alcohols through Visible Light–Promoted Photocatalytic *E* to *Z* Isomerization, *Chem. – Asian J.*, 2020, **15**, 555–559.

12 M. Fagnoni, D. Dondi, D. Ravelli and A. Albini, Photocatalysis for the Formation of the C–C Bond, *Chem. Rev.*, 2007, **107**, 2725–2756.

13 S. Protti and M. Fagnoni, The Sunny Side of Chemistry: Green Synthesis by Solar Light, *Photochem. Photobiol. Sci.*, 2009, **8**, 1499–1516.

14 J. M. Hornback, L. G. Mawhorter, S. E. Carlson and R. A. Bedont, Reactions of O-Xylylenes Produced Photochemically from o-Alkylstyrenes, *J. Org. Chem.*, 1979, **44**, 3698–3703.

15 (*a*) R. G. W. Norrish and C. H. Bamford, Photodecomposition of Aldehydes and Ketones, *Nature*, 1936, **138**, 1016; (*b*) R. G. W. Norrish and C. H. Bamford, Photo-decomposition of Aldehydes and Ketones, *Nature*, 1937, **140**, 195–196; (*c*) R. G. W. Norrish, On The Principle of Primary Recombination in Relation to The Velocity of Thermal Reactions in Solution, *Trans. Faraday Soc.*, 1937, **33**, 1521–1528; (*d*) N. C. Yang and D.-D. H. Yang, Photochemical Reactions of Ketones in Solution, *J. Am. Chem. Soc.*, 1958, **80**, 2913–2914; (*e*) P. J. Wagner, Type II Photoelimination and Photocyclization of Ketones, *Acc. Chem. Res.*, 1971, **4**, 168–177.

16 M. Sayes, G. Benoit and A. B. Charette, Borocyclopropanation of Styrenes Mediated by UV–light Under Continuous Flow Conditions, *Angew. Chem., Int. Ed.*, 2018, **57**, 13514–13518.

17 (*a*) Y. Xia, Y. Liang, Y. Chen, M. Wang, L. Jiao, F. Huang, S. Liu, Y. Li and Z.-X. Yu, An Unexpected Role of a Trace Amount of Water in Catalyzing Proton Transfer in Phosphine-Catalyzed (3 + 2) Cycloaddition of Allenoates and Alkenes, *J. Am. Chem. Soc.*, 2007, **129**, 3470–3471; (*b*) H. Yuan and J. Zhang, $[DBU\text{-}H]^+$ and H_2O as Effective Catalyst Form for 2,3-Dihydropyrido[2,3-*d*]Pyrimidin-4(1 *H*)-Ones: A DFT Study, *J. Comput. Chem.*, 2015, **36**, 1295–1303; (*c*) W. M. C. Sameera, M. Hatanaka, T. Kitanosono, S. Kobayashi and K. Morokuma, The Mechanism of Iron(II)-Catalyzed Asymmetric Mukaiyama Aldol Reaction in Aqueous Media: Density Functional Theory and Artificial Force-Induced Reaction Study, *J. Am. Chem. Soc.*, 2015, **137**, 11085–11094; (*d*) W. Rauf and J. M. Brown, Palladium-Catalysed Directed C–H Activation by Anilides and Ureas; Water Participation in a General Base Mechanism, *Org. Biomol. Chem.*, 2016, **14**, 5251–5257; (*e*) L. Tao, Y. Wei and M. Shi, Thermally–Induced Intramolecular [4 + 2] Cycloaddition of Allylamino– or Allyloxy–Tethered Alkylidenecyclopropanes, *Chem. – Asian J.*, 2021, **16**, 2463–2468.

18 M. J. Frisch, G. W. Trucks, H. B. Schlegel, G. E. Scuseria, M. A. Robb, J. R. Cheeseman, G. Scalmani, V. Barone, G. A. Petersson, H. Nakatsuji, X. Li, M. Caricato, A. V. Marenich, J. Bloino, B. G. Janesko, R. Gomperts, B. Mennucci, H. P. Hratchian, J. V. Ortiz, A. F. Izmaylov, J. L. Sonnenberg, D. Williams-Young, F. Ding, F. Lipparini, F. Egidi, J. Goings, B. Peng, A. Petrone, T. Henderson, D. Ranasinghe, V. G. Zakrzewski, J. Gao, N. Rega, G. Zheng, W. Liang, M. Hada, M. Ehara, K. Toyota, R. Fukuda, J. Hasegawa, M. Ishida, T. Nakajima, Y. Honda, O. Kitao, H. Nakai, T. Vreven, K. Throssell, J. A. Montgomery Jr., J. E. Peralta, F. Ogliaro, M. J. Bearpark, J. J. Heyd, E. N. Brothers, K. N. Kudin, V. N. Staroverov, T. A. Keith, R. Kobayashi, J. Normand, K. Raghavachari, A. P. Rendell, J. C. Burant, S. S. Iyengar, J. Tomasi, M. Cossi, J. M. Millam, M. Klene, C. Adamo, R. Cammi, J. W. Ochterski, R. L. Martin, K. Morokuma, O. Farkas, J. B. Foresman and D. J. Fox, *Gaussian 16, Revision C.01*, Gaussian, Inc., Wallingford CT, 2016.

19 D. Wang, X. Xue, K. N. Houk and Z. Shi, Mild Ring-Opening 1,3-Hydroborations of Non-Activated Cyclopropanes, *Angew. Chem., Int. Ed.*, 2018, **57**, 16861–16865.

20 J. Chen, H. Meng, F. Zhang, F. Xiao and G.-J. Deng, Transition-Metal-Free Selective Pyrimidines and Pyridines Formation from Aromatic Ketones, Aldehydes and Ammonium Salts, *Green Chem.*, 2019, **21**, 5201–5206.